lamellar interfaces. The plot shows a high-calcium augite matrix and low-calcium Opx. Since the analytical technique used has a 300-Å resolution (*5*), the narrow boundary region which includes the Chp margins appears as a near-vertical concentration gradient. The most significant aspect of this plot is the high-calcium node in the augite immediately adjacent to the lamellae. We interpret this node to be due to calcium diffusion away from the lamellae as an expression of growth of the low-calcium margins into the augite matrix.

These data imply that exsolution of Opx lamellae from augite involves two separate steps after the initial nucleation event. The first step is the diffusion of calcium perpendicular to (100) and away from embryonic lamellae, presumed to have nucleated heterogeneously, and with concomitant diffusion of (magnesium and iron) to replace calcium. This initially produces Chp lamellae at least 200 to 300 Å wide. It is assumed that the calcium concentration would be highest at the margins and lowest in the center of these lamellae. The second step consists of glide-twinning inversion (polymorphic with little change in composition) to Opx by the lowest calcium clinopyroxene near the center of the lamellae. The stacking faults in the Opx are believed to represent relict planes where inversion has not occurred, because adjacent regions of Chp have inverted antiphase, and across which the stacking sequence remains locally characteristic of Chp. The strain-induced shear-transformation of Opx to clinopyroxene on (100) is well established (*6*, *7*). The inversion from clinopyroxene to Opx invoked here, however, is related to the exsolution-cooling event and probably represents transformation to a less energetic state. The experimental shear-transformation of Opx to clinopyroxene has been reversed by the annealing of deformed natural materials (*6*) but required temperatures much greater (~ 1000°C) than those needed for the formation of the host augite in this study.

Growth of the lamellae occurs by further diffusion of calcium normal to (100), and thus the process is related to exsolution by simple nucleation and growth. As the leading edges of the low-calcium margins advance into the augite matrix, there occurs the inversion of the trailing edges, which are poorer in calcium than the leading edges. By this process, the margins maintain approximately constant width and the widest lamellae appear to consist entirely of Opx. If lamellar growth continued for an indefinite period, this process would generate optically detectable Opx lamellae with Chp margins remaining suboptical.

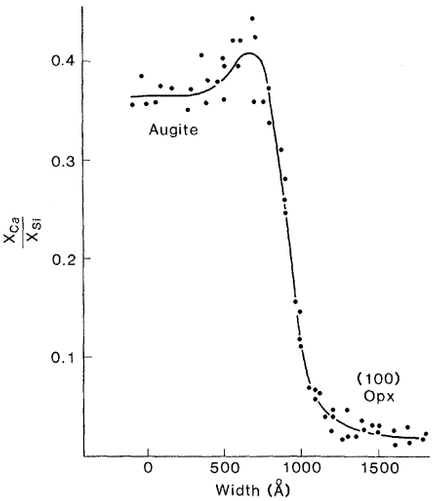

Fig. 2. Concentration profile for calcium relative to silicon across the (100) lamellar interface.

Similar low-calcium Chp margins adjacent to Opx lamellae in augite have been observed in another study but were not interpreted (*8*). The small size of the Chp margins makes them difficult to detect, even with CTEM. This difficulty must in part account for the small number of reported occurrences. However, if the process described above occurs at high temperatures (for example, $\gtrsim$ 1000°C), high rates of diffusion and inversion could result in Chp margins of negligible thickness. In the limit, the two-step process would approach a single step. For these reasons, we suggest that two-step Opx exsolution in augite may be universal.

Petrologic data (*2*) imply that the Opx exsolution event in these rocks occurred during the waning stages of retrograde metamorphism and continued to the lowest temperature at which activation energies for the process could be exceeded. We envision the diffusion-transformation process to have extended over a wide temperature range, with the textures preserved because of a lack of subsequent annealing. The separate energy barrier for nucleation of the initial Chp in augite and the activation energies for lamellar growth by diffusion and subsequent glide transformation to Opx may be significantly less than that for a one-stage exsolution process. This relation may explain why the process apparently continued to relatively low temperatures, where it was preserved.

ANDREW M. ISAACS
Planetary and Earth Sciences Division, NASA Johnson Space Center, Houston, Texas 77058
DONALD R. PEACOR
Department of Geological Sciences, University of Michigan, Ann Arbor 48109

References and Notes

1. W. A. Deer, R. A. Howie, J. Zussman, *Rock Forming Minerals*, vol. 2A, *Single Chain Silicates* (Wiley, New York, 1978).
2. S. R. Bohlen and E. J. Essene, *Contrib. Mineral. Petrol.* **62**, 153 (1977); ———, K. S. Hoffman, *Geol. Soc. Am. Bull.* **91**, 110 (1979).
3. A. M. Isaacs, P. E. Brown, J. W. Valley, E. J. Essene, D. R. Peacor, *Contrib. Mineral. Petrol.* **77**, 115 (1981).
4. S. Iijima and P. R. Buseck, *Am. Mineral.* **60**, 758 (1975).
5. A. M. Isaacs and D. R. Peacor, *Geol. Soc. Am. Abstr. Programs* **13**, 478 (1981).
6. R. S. Coe and S. H. Kirby, *Contrib. Mineral. Petrol.* **52**, 29 (1975).
7. A. C. McLaren and M. A. Etheridge, *ibid.* **57**, 163 (1976).
8. Y. Nakajima and P. H. Ribbe, *Neues Jahrb. Mineral. Monatash.* **6**, 258 (1980).
9. We thank S. R. Bohlen, E. J. Essene, and G. L. Nord, Jr., for valuable suggestions and discussion.

5 April 1982; revised 21 June 1982

Are Ions Involved in the Gating of Calcium Channels?

Abstract. *The rates of activation and deactivation of the currents carried by calcium, strontium, or barium ions through the voltage-sensitive calcium channel of* Paramecium *are different. The differences cannot be attributed to complications due to internal ion concentration, calcium channel inactivation, potassium current activation, surface charge effects, or incomplete space clamping. The findings indicate participation of the divalent cations in the voltage-driven calcium channel gating process.*

Gating, the opening or closing of a voltage-sensitive ion channel, has been viewed as a multistep process corresponding to changes in the conformation or aggregation of the channel molecules. Movements of charges or dipoles correlated with gating by sudden changes in voltage have been measured (*1*). The kinetics of gating must be a reflection of the energy profile traversed by the charges or dipoles. For a given channel, the gating mechanism has been considered to be governed only by the transmembrane voltage and not to be dependent on ions. While the kinetics of inactivation (the fall of current during a voltage step) has been found to be affected by ions in certain calcium, potassium, and sodium channels (*2–4*), the kinetics of activation (the rise of current upon

0036-8075/82/1008-0153$01.00/0

voltage step) or deactivation (the fall of tail current upon repolarization) of the channel has often been considered to be similar in solutions of different ions. However, permeant ions as well as the membrane potential appear to be involved in these gating processes of potassium channels (*5*). We report here that the rates of activation and deactivation of the current through the calcium channel of *Paramecium* are markedly affected by the presence of external Ca^{2+}, Sr^{2+}, or Ba^{2+}.

Paramecium caudatum (Carolina Biological Supply Company) was cultured and rinsed, and specimens were captured and impaled with microelectrodes according to published methods (*6*), with some modification (*7*). They were held at room temperature (19° to 21°C) in a bath containing either Ca solution [1 m*M* $CaCl_2$ in a basic solution of 5 m*M* tetraethylammonium chloride (TEA), 0.5 m*M* KOH, 0.5 m*M* KCl, 1 m*M* Hepes, and 0.01 m*M* EDTA, *p*H 7.3], Sr solution (1 m*M* $SrCl_2$ in the basic solution), or Ba solution (1 m*M* $BaCl_2$ in the basic solution). All experiments were repeated with at least three cells.

In the Ca solution, the resting potential is about −30 mV. The membrane is first voltage-clamped at −40 mV to minimize the inactivation of the Ca channel (*8*). A depolarizing step from the holding to a suprathreshold level induces an inward current (Fig. 1A). This current in the Ca solution rises to a peak within 5 msec and is inactivated in the next ~ 5 msec while the membrane remains depolarized (*9*). The inward current is activated and inactivated more slowly in the Sr solution. In the Ba solution, the current is activated much more slowly and inactivated only slightly, if at all. We believe that the Ca, Sr, and Ba currents are through the same channel in *Paramecium* because mutations (*10*), deciliation (*11*), or channel blockers (*12*) that abolish the Ca current also abolish the Sr and Ba currents. The time to peak of the inward current, plotted against the voltage step in the three solutions in Fig. 1B, is shortest for the Ca current and longest for the Ba current.

The decrease of the current after the peak has been ascribed to inactivation of the Ca channel by internal Ca^{2+}. Neither Ba^{2+} nor Sr^{2+} is as effective as Ca^{2+} in this inactivation (*13*). The slow peaking of the Ba current might be attributed to this ineffectiveness. However, removal of a large part of the inactivation of the Ca current by injection of $EGTA^{2-}$ does not significantly alter the time to peak, which remains much shorter than that of the Ba current (Fig. 1D) (*3*). Thus the peak time is largely independent of inactivation.

The difference in activation of currents in Ca^{2+}, Sr^{2+}, and Ba^{2+} is not a result of changes in K channel activation. First, all the solutions contain 5 m*M* TEA, which suppresses the delayed K^+ current (*14*). Second, the difference in activation appears even when the depolarization is too small for the K activation, which has a threshold ~ 15 mV more depolarized than that of the Ca activation (*15*).

The difference in activation in different

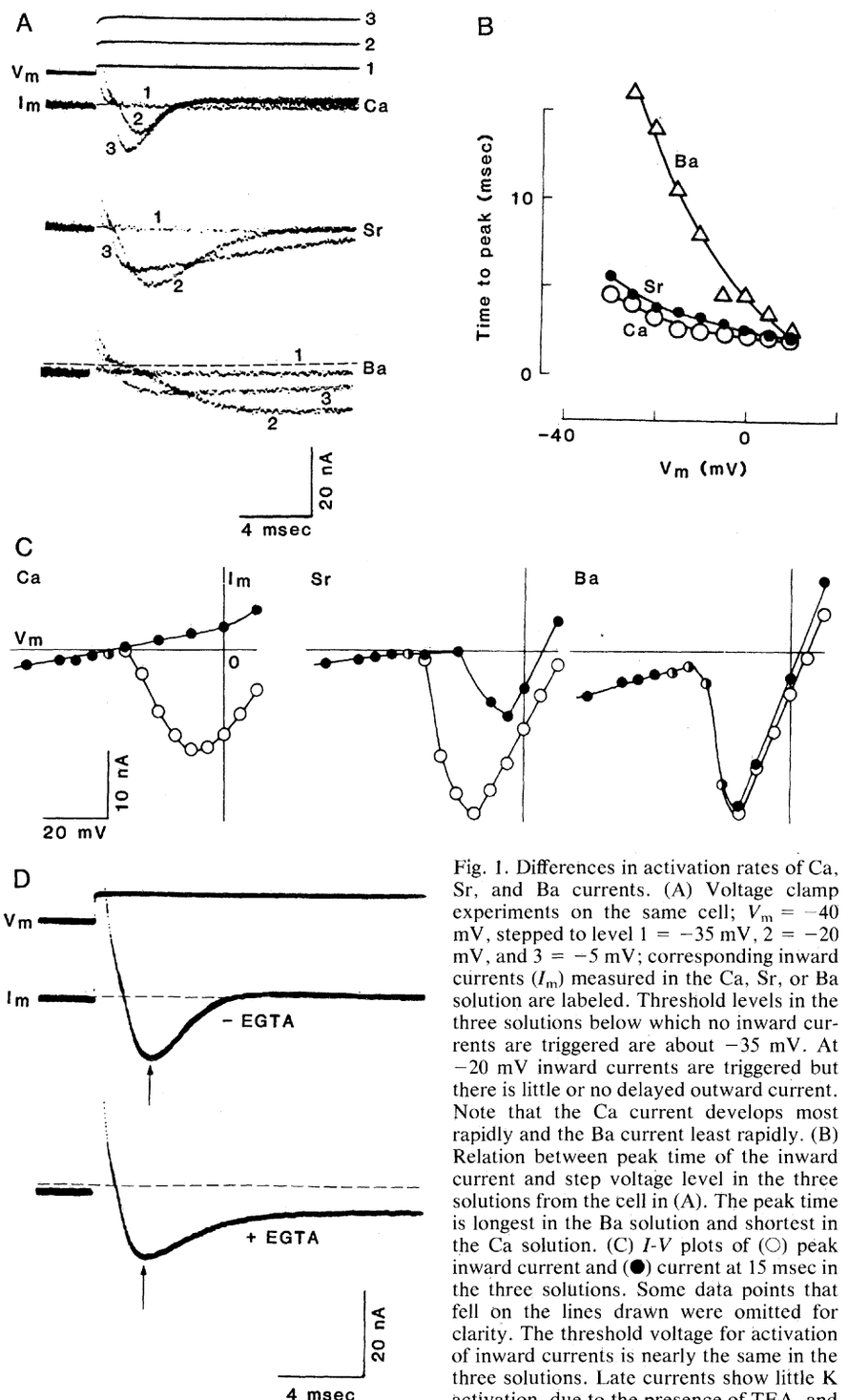

Fig. 1. Differences in activation rates of Ca, Sr, and Ba currents. (A) Voltage clamp experiments on the same cell; V_m = −40 mV, stepped to level 1 = −35 mV, 2 = −20 mV, and 3 = −5 mV; corresponding inward currents (I_m) measured in the Ca, Sr, or Ba solution are labeled. Threshold levels in the three solutions below which no inward currents are triggered are about −35 mV. At −20 mV inward currents are triggered but there is little or no delayed outward current. Note that the Ca current develops most rapidly and the Ba current least rapidly. (B) Relation between peak time of the inward current and step voltage level in the three solutions from the cell in (A). The peak time is longest in the Ba solution and shortest in the Ca solution. (C) *I-V* plots of (○) peak inward current and (●) current at 15 msec in the three solutions. Some data points that fell on the lines drawn were omitted for clarity. The threshold voltage for activation of inward currents is nearly the same in the three solutions. Late currents show little K activation, due to the presence of TEA, and incomplete inactivation of the Sr and Ba currents. (D) Lack of effect of $EGTA^{2-}$ injection on activation rate of the Ca current. The $EGTA^{2-}$ was injected under voltage clamp with a 10^{-8} A current for 3 minutes through a third electrode filled with 100 m*M* potassium EGTA and 100 m*M* Hepes (*p*H 7.0). The injected $EGTA^{2-}$ reduces current inactivation after the peak but has no effect on activation time course and peak time (arrows). Upper frame, before $EGTA^{2-}$ injection; lower frame, same cell after the injection. Currents were induced by a step from −40 to −10 mV. Interrupted lines refer to zero current levels.

solutions also cannot be explained by possible differential effects of Ca^{2+}, Sr^{2+}, or Ba^{2+} on surface charges (*16*). First, the threshold potential for activation of the Ca channel is nearly the same in the three solutions (Fig. 1C); the difference, if any, is less than 5 mV in all cases. Second, the voltage at which the Sr and Ba currents become maximal is at most 10 mV more negative than that for the Ca current (Fig. 1C). If this means that Ba^{2+} and Sr^{2+} are less effective in neutralizing the surface charge, the apparent voltage sensitivity of the Ca channel in the Sr or Ba solution should be 10 mV more negative than in the Ca solution. The time for the Ca current to reach its peak remains much shorter than the time for the Sr or Ba current, even when the latter are induced by voltage steps of the same size but from a holding level that is 10 mV more negative. Third, the Sr activation is clearly faster than the Ba activation (Fig. 1), although the current-voltage (*I-V*) relations in the two solutions are nearly identical. Furthermore, changing the Ca^{2+} concentration over the range 0.38 to 5.60 m*M* shifts the *I-V* curve by 40 mV in the membrane of *P. tetraurelia* without a significant change in the activation time course of the Ca current (*15*). Therefore, we conclude that the differences in rate of activation (Fig. 1A) or time to peak (Fig. 1B) of the inward currents in the different ion solutions reflect alterations in the rate of Ca channel activation; that is, the opening of the Ca channel is ion-dependent.

The deactivation of the channel population is reflected by the tail current upon a downward step of the voltage after a depolarization. The tail current (*17*) through the Ca channel shows an exponential decay (Fig. 2, A and B). The deactivation time courses of the Ca, Sr, and Ba tail currents in each solution are clearly different. The time constants (τ's) of the three tail currents upon repolarization to the holding level (−40 mV), calculated from linear regressions of semilogarithmic plots of current versus time, are 0.29 ± 0.03 msec (mean ± standard deviation; $N = 7$), 0.55 ± 0.11 msec ($N = 4$), and 0.86 ± 0.24 msec ($N = 3$), respectively. Although measurements of τ for the fast Ca tail may be partly masked by the capacitative surge [the τ of this surge estimated with ~ 20-mV hyperpolarizations is 0.19 ± 0.05 msec ($N = 9$) in all solutions], the Ca tail current decays fastest, followed by the Sr tail and then the Ba tail. As predicted for voltage-dependent closure of channels, the more negative level the membrane steps back to, the faster the deactivation. The τ's are 0.25 ± 0.05 msec ($N = 7$), 0.30 ± 0.04 msec ($N = 4$), and 0.35 ± 0.08 msec ($N = 3$), respectively, when stepped back to −50 mV (*18*).

The τ's in a given solution are nearly the same regardless of the degree of prior activation of the Ca channel by changes in the size or duration of the depolarization step. Also, the amplitude of the tail current saturates as the depolarization step increases in size. These observations indicate that the τ's reflect the true decay of the current through the Ca channel (*19*) and not some artifact due to possible unclamped ciliary space (*20*), since clamp complication should be more severe when the voltage step is larger.

That the time constants of the tails are largely independent of the internal concentration of divalent cation is indicated by two-pulse experiments in the Sr solution of the type described by Brehm and Eckert (*13*) (Fig. 2C). A first pulse with variable step size is followed by a constant second pulse after a fixed interval. The second inward current and the tail current associated with repolarization to the holding level are examined. Both the peak amplitude and the tail amplitude of the second Sr current decrease as the first voltage step is increased to ~ 0 mV. Above this voltage, both the inward current and its tail associated with the second pulse increase. As the first voltage step approaches the Sr^{2+} equilibrium potential, there is apparently less intracellular accumulation of Sr^{2+} and thus less inactivation of the Ca channel by internal Sr^{2+} when the inward current is examined with the second pulse (*13*). Although the tail currents change in size, their time constants are not altered by the size of the first voltage step (Fig. 2C). Similar results were obtained in the Ba solution.

The differences in rates of activation and deactivation of the Ca, Sr, and Ba currents indicate that the gating mecha-

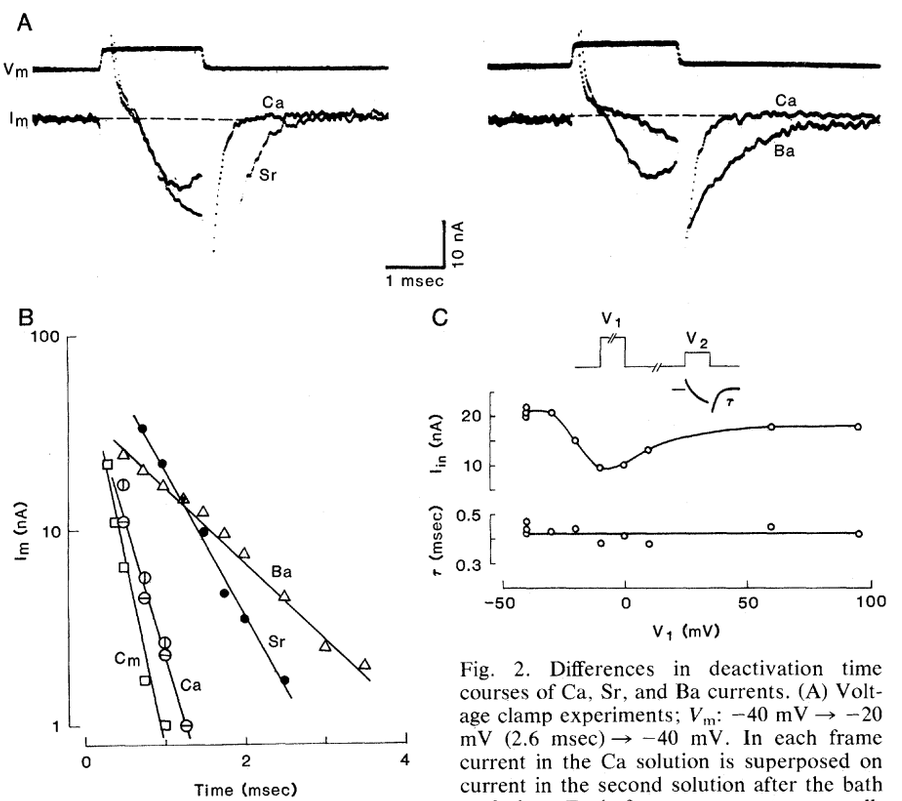

Fig. 2. Differences in deactivation time courses of Ca, Sr, and Ba currents. (A) Voltage clamp experiments; V_m: −40 mV → −20 mV (2.6 msec) → −40 mV. In each frame current in the Ca solution is superposed on current in the second solution after the bath perfusion. Each frame represents one cell. Note that the tail current, identified by the element symbols nearby, decays most slowly in the Ba and most rapidly in the Ca solution. (The Ca current during the step is the one that shows inactivation in these experiments.) Contamination by capacitative current (I_c) is minimal after 0.5 msec of the step, as evidenced by the outward I_c preceding the inward current. The Sr current at 2.6 msec is much larger than the Ca or the Ba current (Fig. 1A). Correspondingly, the Sr tail starts with a larger value, and its earlier part is not shown in order to accommodate the rest of the figure. (B) Semilogarithmic plots of tail currents induced by the above voltage step against time. Points ⊕ and △ represent one cell and ⊖ and ● represent another; C_m (□) is the maximal I_c induced in these two cells by 20-mV hyperpolarization. (C) Two-pulse experiments in the Sr solution, showing that the inward current but not the deactivation rate of the tail is affected by the internal concentration of ion. V_m: −40 mV → various V_1 (20 msec) → −40 mV (40 msec) → fixed V_2 (−20 mV, 4 msec) → −40 mV, as shown, for measurements of τ of the tails; or → V_2, −20 mV (40 msec), not shown, for measurements of peak inward currents (I_{in}) associated with V_2. Note that I_{in} more than halved near the midrange of V_1 due to internal accumulation of Sr^{2+}, but little or no change in τ is seen throughout the V_1 range.

nism of the *Paramecium* Ca channel (*21*) is not only voltage-sensitive but also ion-dependent. The site or sites at which these ions exert their effect must be accessible from the outside, because activation of the Ca channel must precede the ion flux and is altered by external ions in our experiments.

It is not clear whether ions, permeant or impermeant, are involved in the gating of voltage-sensitive channels in general, although recent studies of K channels suggest this (*5*). The gating of the Na channel seems to be affected by Zn^{2+}, and Ni^{2+} and possibly Ca^{2+} or Mg^{2+} (*22*). Whether the presence of Ca^{2+} or another divalent cation affects gating currents of the Ca channel (*23*) has not been tested directly. Changes in the rate of Ca channel activation or deactivation have been noted in an insect muscle, *Helix* neuron, and frog muscle (*4, 19*).

If the gating process is viewed as involving conformational changes of the channel that is accessible to ions, it is not surprising that there is an interaction between the gating charges and the ions. The situation may be analogous to the substrate- or cofactor-enzyme interaction involved in changes of enzyme conformation.

YOSHIRO SAIMI
CHING KUNG
Laboratory of Molecular Biology and *Department of Genetics, University of Wisconsin, Madison 53706*

References and Notes

1. C. M. Armstrong, *Physiol. Rev.* **61**, 644 (1981).
2. H. Meves and W. Vogel, *J. Physiol. (London)* **235**, 225 (1973); R. Eckert and D. Tillotson, *ibid.* **314**, 265 (1981); P. R. Stanfield, F. M. Ashcroft, T. D. Plant, *Nature (London)* **289**, 509 (1981).
3. P. Brehm, R. Eckert, D. Tillotson, *J. Physiol. (London)* **306**, 193 (1981).
4. F. M. Ashcroft and P. R. Stanfield, *Science* **213**, 224 (1981); A. M. Brown, K. Morimoto, Y. Tsuda, D. L. Wilson, *J. Physiol. (London)* **321**, 193 (1981).
5. S. Hagiwara, S. Miyazaki, S. Krasne, S. Ciani, *J. Gen. Physiol.* **70**, 269 (1977); S. Ciani, S. Krasne, S. Miyazaki, S. Hagiwara, *J. Membr. Biol.* **44**, 103 (1978); R. P. Swenson and C. M. Armstrong, *Nature (London)* **291**, 427 (1981); G. A. Leech and P. R. Stanfield, *J. Physiol. (London)* **319**, 295 (1981).
6. T. M. Sonneborn, in *Methods of Cell Physiology*, D. M. Prescott, Ed. (Academic Press, New York, 1970), p. 469; Y. Naitoh and R. Eckert, *Exp. Physiol. Biochem.* **5**, 17 (1972).
7. A reference electrode was placed near the cell, except when replaced with the iontophoresis electrode. An inverted microscope was used to allow electrode access from above with a short submersion length. The time constant of the *I-V* converter was < 100 μsec; the open-loop gain of the feedback circuit $\simeq \times 250$; and the series resistance to the cell < 90 kilohms with and < 200 kilohms without the reference electrode; electrodes were filled with 3*M* KCl with resistance < 20 megohms.
8. None or less than 10 percent of the Ca conductance was inactivated at this holding level.
9. D. Oertel, S. Schein, C. Kung, *Nature (London)* **268**, 120 (1977); R. Eckert and P. Brehm, *Annu. Rev. Biophys. Bioeng.* **8**, 353 (1980).
10. C. Kung and R. Eckert, *Proc. Natl. Acad. Sci. U.S.A.* **69**, 93 (1972).
11. K. Dunlap, *J. Physiol. (London)* **271**, 119 (1977); A. Ogura and K. Takahashi, *Nature (London)* **264**, 170 (1976).
12. Y. Saimi, unpublished results.
13. P. Brehm and R. Eckert, *Science* **202**, 1203 (1978).
14. Y. Saimi, in preparation. The 5 m*M* TEA suppresses the delayed K current up to 75 percent in the Ca solution. The remaining outward current appears to be larger in the Sr and Ba solutions, which should have hastened rather than delayed the apparent fall of the inward current.
15. C. Kung and Y. Saimi, *Annu. Rev. Physiol.* **44**, 519 (1982); Y. Satow and C. Kung, *J. Exp. Biol.* **74**, 149 (1979).
16. L. Byerly and S. Hagiwara, *J. Physiol. (London)* **322**, 503 (1982).
17. The current change after 0.5 msec was measured and taken as the tail current because of the capacitative surge (see text).
18. The differences in the τ's of the tail currents in our three solutions cannot be accounted for by the possible differences in surface charge. First, comparison of the τ's in the Ca solution at -35 mV and in the Sr or Ba solution at -45 mV [the maximum possible difference attributable to surface charge is ~ 10 mV as judged by the *I-V* relations of Ca versus Sr or Ba inward currents (Fig. 1C)] reveals that the τ's of Sr or Ba tails remain larger than that of the Ca tail. Second, the *I-V* relations in the Sr and Ba solutions are identical, while the τ for the Ba tail is larger than that for the Sr tail (see text).
19. W. Almers and P. T. Palade, *J. Physiol. (London)* **312**, 159 (1981).
20. S. Hagiwara and L. Byerly, *Annu. Rev. Neurosci.* **4**, 69 (1981).
21. We estimated that four or five gating particles were involved in the Ba^{2+} current, assuming there is little inactivation of this current. Y. Naitoh (unpublished results) found five particles for the Ca^{2+} current. Therefore, the basic gating process appears to be the same in various solutions, but the rate constants seem to be different.
22. B. Frankenhaeuser and A. L. Hodgkin, *J. Physiol. (London)* **137**, 218 (1957); F. Bezanilla and C. M. Armstrong, *Science* **183**, 753 (1974); H. Meves, *J. Physiol. (London)* **254**, 787 (1976); C. M. Armstrong and F. Bezanilla, *Ann. N.Y. Acad. Sci.* **264**, 265 (1975); C. M. Armstrong and W. F. Gilly, *J. Gen. Physiol.* **74**, 691 (1979); F. A. Dodge, in *Biophysics of Physiological and Pharmacological Actions*, A. M. Shanes, Ed. (AAAS, Washington, D.C., 1961), p. 119; B. Hille, *J. Gen. Physiol.* **51**, 221 (1968); M. P. Blaustein and D. E. Goldman, *ibid.*, p. 279.
23. D. J. Adams and P. W. Gage, *J. Physiol. (London)* **289**, 115 (1979); P. G. Kostyuk, O. A. Krishtal, V. I. Pidoplichko, *ibid.* **310**, 403 (1981).
24. We are very grateful for critical readings of the manuscript and valuable comments to J. W. Deitmer, R. Eckert, M. Epstein, D. Oertel, and A. O. Stretton. Supported by NSF grants BNS 79-18554 and PHS GM22714.

23 February 1982; revised 14 June 1982

Bilirubin-Induced Modulation of Cerebral Protein Phosphorylation in Neonate Rabbits in vivo

Abstract. *Protein phosphorylation in cerebral cell-free preparations from neonate rabbits was inhibited by bilirubin and promoted by aminophylline when these substances had been administered intravenously. In animals given both compounds, the bilirubin-induced inhibition of phosphorylation was partly reversed by aminophylline. Adenosine 3′,5′-monophosphate added in vitro during the assays also increased protein phosphorylation. These data introduce new concepts in the pathogenesis of kernicterus.*

Kernicterus is a complication of severe unconjugated hyperbilirubinemia confined almost entirely to the neonatal period. Even though the disease has been studied at the molecular level, the major biochemical defect underlying bilirubin encephalopathy has yet to be determined. Bilirubin inhibits oxidative processes in isolated mitochondria, suggesting that it exerts its cytotoxic effect in the kernicteric brain by diminishing local adenosine triphosphate (ATP) levels, thus leading eventually to impairment of energy-dependent cerebral metabolism (*1*).

The report that bilirubin in vitro inhibits its adenosine 3′,5′-monophosphate (cyclic AMP)–dependent protein kinase activity with purified histone as the substrate has introduced new concepts in the mechanism of pathogenesis of kernicterus (*2*). Yet, unequivocal linkage of this action of bilirubin to the pathogenesis of bilirubin-induced encephalopathy requires demonstration of a similar effect in vivo.

Protein phosphorylation was studied in the cerebrum of neonate rabbits after they were given bilirubin or aminophylline, or both, intravenously at various doses in 1 ml of solvent. An attempt was made to evaluate the effect of bilirubin on the overall estimation of protein phosphorylation. In addition, the individual contributions from cyclic AMP–dependent as well as cyclic AMP–independent routes of phosphorylation were examined.

The experiments were carried out in three groups of animals: those in group A were treated with bilirubin (Sigma); those in group B received aminophylline (theophylline and ethylenediamine; Cooper); and those in group C were injected with aminophylline (2 mg per 100 g of body weight, intravenously) 30 minutes after the administration of various doses of bilirubin. Rabbits were of both sexes, 3 to 4 days old, and weighed 65 to 90 g each; they were decapitated 30 minutes after bilirubin or aminophylline administration. Cerebrum homogenates were centrifuged (30,000*g* for 20 minutes), and supernatants in phosphate buffer (0.05*M*, *p*H 7) were used as the source of the enzyme. Protein phosphorylation determined (*3*) with purified histone (fraction II-A, Sigma) as the substrate, was expressed as picomoles of ^{32}P-labeled inorganic phosphate ($^{32}P_i$) from [γ-^{32}P]ATP

0036-8075/82/1008-0156$01.00/0